

PROTOTYPE OF AN INTER-DIGITAL H-MODE DRIFT-TUBE LINAC FOR MUON LINAC

Y. Nakazawa*, H. Iinuma, Ibaraki University, Mito, Ibaraki, Japan

Y. Iwata, National Institute of Radiological Sciences, Chiba, Japan

Y. Iwashita, Kyoto University, Kyoto, Japan

M. Otani, N. Kawamura, T. Mibe, T. Yamazaki, M. Yoshida, KEK, Tsukuba, Ibaraki, Japan

R. Kitamura, H. Yasuda, University of Tokyo, Hongo, Tokyo, Japan

Y. Kondo, K. Hasegawa, T. Morishita, JAEA, Tokai, Naka, Ibaraki, Japan

N. Saito, J-PARC center, Tokai, Naka, Ibaraki, Japan

Y. Sue, Nagoya University, Nagoya, Japan

N. Hayashizaki, Tokyo Institute of Technology, Tokyo, Japan

Abstract

An inter-digital H-mode (IH) drift-tube linac (DTL) is developed for a low velocity part in a muon linac at the J-PARC E34 experiment. It will accelerate muons from $\beta = 0.08$ to 0.28 at an operational frequency of 324 MHz. In order to achieve higher acceleration efficiency and make cost lower, an alternative phase focusing (APF) scheme is adopted. A prototype with 6 cells of 0.45 m length was manufactured. The prototype accelerates muons from $\beta = 0.08$ to 0.15 stage. We conducted frequency measurement and bead-pull measurement as a low-power measurement, in order to evaluate the prototype product. In this paper, the results of the low-power measurement for prototype cavity will be presented.

INTRODUCTION

The muon anomalous magnetic moment ($g-2$) is the one of the promising signals of beyond the Standard Model. The E821 experiment at Brookhaven National Laboratory found the 3.7σ discrepancy between the SM theoretical calculation and the measurement of the muon $g-2$ [1, 2]. The muon beam in the E821 experiment was produced by in-flight pion decay with large emittance, which requires electric quadrupoles to keep the muon beam inside of the beam pipe. In order to avoid muon precession in the electric field, the muon beam should be well adjusted to the fixed value (magic momentum).

In the case of J-PARC experiment (J-PARC E34), we plan to measure muon $g-2$ and EDM (Electric Dipole Moment) with new technique [3]. We will provide a low emittance muon beam for high precision measurement from the stopping pion decay and their reacceleration steps [4]. In this method, electric field is not needed in storage ring, and the systematic error is reduced.

Figure 1 shows the schematic image of muon linac. μ^+ with a kinetic energy of 30meV called ultra slow muon (USM) is accelerated by muon linac. The muon linac is composed of a radio frequency quadrupole (RFQ) linac, the IH-DTL, a disc and washer coupled cavity linac (DAW-

CCL), and a disc loaded structure (DLS). The USM is accelerated to 212 MeV. The IH-DTL is employed during the particle velocity $\beta = 0.08$ to 0.28 stage with an operational frequency of 324 MHz.

In this paper, we describe the result of the low-power measurement of the prototype cavity. The paper is structured as follows. First the prototype design is described. Next, the results and discussion of frequency measurement and bead-pull measurement is presented. Finally, the summary is presented.

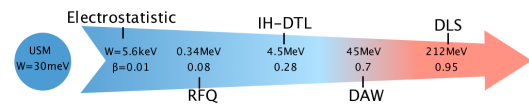


Figure 1: Schematic image of muon linac.

APF IH-DTL

H-mode DTL is installed hollow conducting drift tube along the beam axis. The drift tube is supported by stems attached to the outer wall. In time variation, the magnetic fields at the surface of the stems induce current. The structure of IH-DTL prototype is shown in Fig. 2. The IH cavity consists of two ridges arranged on both the top and bottom sides of the cavity. Five drift tubes are arranged alternately on the top and bottom via stems on the ridges, in order to excite TE_{11} -mode. The beams are accelerated by the longitudinal electric field with the gap.

The focusing section is necessary for linac to suppress the beam dispersion. The usual focusing method is provided by a quadrupole magnet and a permanent magnet. However, our IH-DTL employs the alternating phase focusing (APF) method [5, 6]. In APF method, the focusing or divergence of beam is controlled with the RF field only by optimizing synchronous phase of gap. Thus, the IH structure is simplification and is able to be fabricated at lower cost.

The motion equation of the longitudinal and transverse focusing in RF field are expressed as

$$z'' - \frac{\pi e E_0 T \sin \phi}{2m_0 c^2 \beta^3 \gamma^3 \lambda} z = 0 \quad (1)$$

* 18nm021f@vc.ibaraki.ac.jp

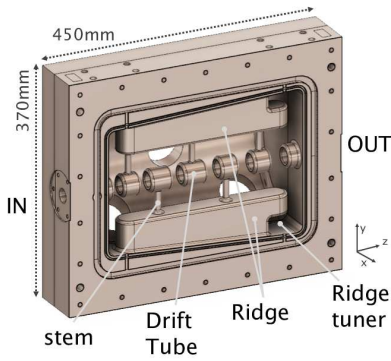


Figure 2: Sectional view of IH-DTL prototype in 3D model.

$$r'' + \frac{\pi e E_0 T \sin \phi}{2m_0 c^2 \beta^3 \gamma^3 \lambda} r = 0 \quad (2)$$

where E_0 is the unperturbed electric field, T Transit time factor, γ Lorentz factor, λ RF wave length, and ϕ is the synchronous phase [7, 8]. Equations (1) and (2) show that negative synchronous phase provides longitudinal focusing and transverse defocusing, and positive synchronous phase provides longitudinal defocusing and transverse focusing. Hence, we are able to control the longitudinal and transverse focusing by optimizing the gap-to-gap synchronous phases.

For APF method, an acceleration and the focusing are achieved with the RF field only. In order to optimize the cavity structure, synchronous phase array optimization, cavity optimization, and particle tracking are required. The prototype design is determined by the actual cavity optimization. The actual cavity is calculated [9] and has 16 cells and the cavity length is approximately 1.3 m to correspond to approximately 4 MeV. The 1–6 cells of the actual cavity are in the prototype cavity [10]. We calculated the electromagnetic field in the prototype cavity by using the CST Micro Wave (MW) Studio [11]. Table 1 shows the cell parameters of the prototype cavity optimization. The prototype cavity is employed during the particle velocity $\beta = 0.08$ to 0.28 stage.

Moreover, the beam particle trajectory was calculated by using general particle tracer (GPT) [12]. The most precise evaluation of the output beam can be obtained using realistic input beam distributions. The input beam was used muon beam that the normalized root mean square (rms) emittances of the input beam were evaluated as $\varepsilon_x = 0.297\pi$ mm mrad in the x -direction, $\varepsilon_y = 0.168\pi$ mm mrad in the y -direction. This beam was simulated from the surface muon beam line, the USM system, and the RFQ acceleration [13]. The output beam of the normalized emittance (and emittance growth) was calculated to be $\varepsilon_x = 0.312\pi$ mm mrad (+5.1%) and $\varepsilon_y = 0.182\pi$ mm mrad (+8.2%) in the x -direction and y -directions, respectively.

FREQUENCY MEASUREMENT

Prior to bead-pull measurement, we estimated the resonant frequency and an unloaded Q (Q_0) in prototype cavity

Table 1: Cell Parameters for Optimized Phase Array

Cell	W [MeV]	β	ϕ [degree]
1	0.34	0.08	-35.9
2	0.43	0.09	-14.9
3	0.57	0.10	12.9
4	0.74	0.12	32.9
5	0.92	0.13	15.4
6	1.14	0.15	-13.8
exit	1.3		

by measuring the scattering parameters. First, the cavity frequency and coupling constant β were measured in reflection (S_{11} and S_{22}). This was done with a vector network analyzer (VNA) coupled to two RF pick-up loops as cavity probes. Next, the resonant frequency and a loaded Q (Q_L) were measured in transmission measurement (S_{21}). Then, the Q_0 was calculated by the measured β and the Q_L . Table 2 shows a comparison of the designed value with the measured value by VNA.

Table 2: Frequency Measurement

	Simulation	Measurement
Resonant frequency [MHz]	321.53	321.21
Q_L (loaded Q)	-	6125.8
β_1	-	0.075
β_2	-	0.1814
Q_0 (unloaded Q)	8700	7695.2

BEAD-PULL MEASUREMENT

Slater Perturbation Theorem

According to the Slater perturbation theorem for electromagnetic field in cavity, the resonant frequency is shifted, when a small volume like a bead is removed from the cavity volume [14]. The shift of the resonant frequency depends on the relative strengths of the electric field and the magnetic field. For a spherical perfectly conducting bead of radius r , the shift given as a function of the unperturbed field amplitudes E_0 and H_0 , by

$$\frac{f_p - f_0}{f_0} = -\frac{\pi r^3}{U} \left[\varepsilon_0 E_0^2 - \frac{\mu_0 H_0^2}{2} \right] \quad (3)$$

where f_p is the perturbed frequency, f_0 is the unperturbed frequency U is the stored energy in cavity, ε_0 is the permittivity of vacuum, and μ_0 is the permeability of vacuum [15].

Instead of measuring the shift of frequency, the shift of the phase has been measured and then translated it into frequency-shift by

$$\frac{f_p - f_0}{f_0} = \frac{\tan(\Delta\phi)}{2Q_L} \quad (4)$$

where $\Delta\phi(= \phi_p - \phi_0)$ is the phase-shift derived from the unperturbed phase and the perturbed phase.

Experimental Setup

Figure 3 shows the experimental setup for bead-pull measurement. In the experiments, we used the aluminum bead with a 1.5 mm radius assumed the spherical perfectly conducting bead. The bead is attached to a non-conducting wire (fishing line) that is driven through the IH cavity.

The stepping motor was controlled by stored program controller and was used to move the bead and the wire on the beam axis. In this time, the position of bead is in beam axis with an uncertainty of 2 mm.

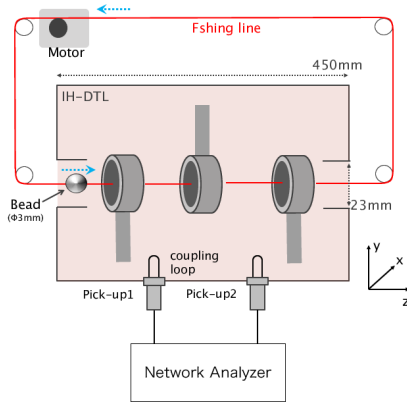


Figure 3: Experimental setup for bead measurement.

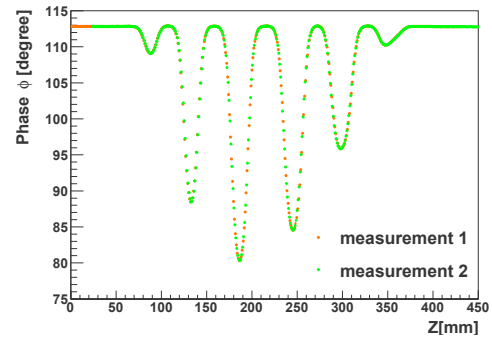
Result & Discussion

The phase of S_{21} at the unperturbed frequency was measured by the VNA. Figure 4(a) shows the plot of phase in cavity versus bead position, when the bead traveled between incident port and outgoing port as measurement 1 and measurement 2, respectively. The measurement 1 was consistent with the measurement 2 with an uncertainty of 1%. The baseline of unperturbed phase is 113 degrees. The six phase-shifts derived from the perturbation was measured in IH cavity.

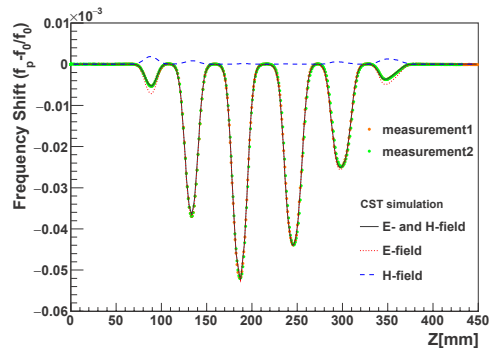
Figure 4(b) shows the dependence of frequency-shift converted by using the measured phase shift and Eq. (4) on the bead position with overwriting of the electromagnetic field (right side of Eq. (3)), E field (the first term on the right side of Eq. (3)), and H field (the first second on the right side of Eq. (3)) by CST.

For IH cavity, there is the magnetic field on the beam axis. In order to confirm whether to be excited the designed accelerating electric field, it is necessary to consider the electromagnetic field in bead-pull measurement. As a result of Fig. 4(b), the measured value is consistent with the simulated value of the field with an uncertainty of 3%.

The cause of the uncertainty is systematic error by mismatching beam axis of bead. We estimated the variation of electric field distribution by CST, when the bead deviated from beam axis in the transverse directions. The variation of



(a)



(b)

Figure 4: (a) Phase shift ($\Delta\phi$) measurement 1 (or 2) as a function z -axis, when bead is moved from incident (outgoing) port to outgoing (incident) port. (b) A comparison between frequency shift by measurement and E and H field (Solid line), E field and H field (dotted line) as a function z .

accelerating electric field is approximately 2–3% at the position located in transverse direction of 3 mm from the beam axis. The bead is located in beam axis with an uncertainty of 2 mm. Therefore, we verified that the electromagnetic field of prototype cavity is consistent with the simulated field within the systematic error.

SUMMARY

In this paper, the prototype cavity was evaluated for studying the actual cavity of IH-DTL in J-PARC g-2/EDM experiment. The resonant frequency and Q_0 in cavity were estimated by measuring the scattering parameters. Moreover, the electric and magnetic field of prototype cavity was measured by bead-pull measurement. As a result, we confirmed the electromagnetic field distribution of prototype cavity is consistent with the simulated field by CST. The prototype cavity was manufactured as intended.

ACKNOWLEDGMENT

This work is supported by JSPS KAKENHI Grant Numbers JP15H03666, JP18H03707, JP16H03987, and JP16J07784.

REFERENCES

- [1] G. W. Bennett *et al.*, *Phys. Rev.*, vol. D73, pp. 072003, 2006.
- [2] A. Keshavarzi *et al.*, *Phys. Rev.* vol. D 97, pp. 114025, 2018.
- [3] T. Mibe *et al.* edit., *J-PARC E34 Conceptual Design Report, Technical Design Report*, 2011.
- [4] Y. Kondo *et al.*, “Re-Acceleration of Ultra Cold Muon in JPARC Muon Facility”, in *Proc. IPAC’18*, Vancouver, BC, Canada, Apr./May 2018, pp. 5041–5046. doi:10.18429/JACoW-IPAC2018-FRXGBF1
- [5] S. Minaev, U. Ratzinger, and B. Schlitt, “APF or KONUS drift tube structures for medical synchrotron injectors – A comparison”, in *Proc. PAC’99*, New York, NY, USA, pp. 3555–3557, 1999.
- [6] Y. Iwata *et al.*, “Alternating-phase-focused IH-DTL for an injector of heavy-ion medical accelerators”, *Nucl. Instrum. Methods Phys. Res.*, Sect. A, vol. 569, pp. 685, 2006.
- [7] T. Hata *et al.*, in *Proc. of the 26th Linear Accelerator Meeting in Japan*, pp. 186-188, 2001.
- [8] J. Pang, L. Zhao, X. He, and Z. Ying, “Progress of An Interdigital H-mode Drift-Tube-Linac with low injection energy”, *PACS 29.20.Ej*; 41.75.-i, 2010.
- [9] M. Otani *et al.*, “Interdigital H-mode drift-tube linac design with alternative phase focusing for muon linac”, *Phys. Rev. Accel. Beams*. vol. 19, pp. 040101, 2016.
- [10] N. Hayashizaki and M. Yoshida, “Development of low energy muon linac”, in *Proc. of the 11th Annual Meetings of Particle Accelerator Society of Japan* Particle Accelerator Society in Japan, Tokyo, Japan, paper SUP043, Aug. 2014.
- [11] CST Studio Suite, Computer Simulation Technology (CST), <https://www.cst.com/products/CSTMWS>
- [12] General Particle Tracer, Pulsar Physics, <http://www.pulsar.nl/gpt/>
- [13] Y. Kondo *et al.*, “Simulation study of muon acceleration using RFQ for a new muon g-2 experiment at J-PARC”, in *Proc. IPAC’15*, Richmond, VA, USA, May 2015, pp. 3801–3803. doi:10.18429/JACoW-IPAC2015-THPF045
- [14] Sumit Som *et al.*, “Bead-Pull Measurement Using Phase-Shift Technique In Multi-Cell Elliptical Cavity”; in *Proc. IPAC’11*, San Sebastian, Spain, Sep. 2011, paper MOPC088, pp. 280–282.
- [15] Thomas P. Wangler, *RF Linear Accelerators*, 2008, Wiley-VCH Verlag GmbH&Co.